Biogeosciences Discuss., doi:10.5194/bg-2016-377, 2016
Manuscript under review for journal Biogeosciences
Published: 16 September 2016

Biogeosciences Discussions Open Access EGU

Transient Dynamics of Terrestrial Carbon Storage: Mathematical foundation and Numeric Examples

Yiqi Luo[1,2], Zheng Shi[1], Xingjie Lu[3], Jianyang Xia[4], Junyi Liang[1], Jiang Jiang[1], Ying Wang[5], Matthew J. Smith[6], Lifen Jiang[1], Anders Ahlström[7, 8], Benito Chen[9], Oleksandra Hararuk[10], Alan Hastings[11], Forrest Hoffman[12], Belinda Medlyn[13], Shuli Niu[14], Martin Rasmussen[15], Katherine Todd-Brown[16], Ying-Ping Wang[3]

[1]Department of Microbiology and Plant Biology, University of Oklahoma, Norman, Oklahoma, USA, [2]Center for Earth System Science, Tsinghua University, Beijing, China, [3]CSIRO Oceans and Atmosphere, Aspendale, Victoria, Australia, [4]School of Ecological and Environmental Sciences, East China Normal University, Shanghai, China, [5]Department of Mathematics, University of Oklahoma, Norman, Oklahoma, USA, [6]Computational Science Laboratory, Microsoft Research, Cambridge, UK, [7]Department of Earth System Science, Stanford University, Stanford, California, USA, [8]Department of Physical Geography and Ecosystem Science, Lund University, Lund, Sweden, [9]Department of Mathematics, University of Texas, Arlington, TX, USA, [10]Pacific Forestry Centre, Canadian Forest Service, Victoria, British Columbia, Canada, [11]Department of Environmental Science and Policy, University of California, One Shields Avenue, Davis, CA 95616, USA, [12]Computational Earth Sciences Group, Oak Ridge National Laboratory, Oak Ridge, TN 37831, USA, [13]Hawkesbury Institute for the Environment, Western Sydney University, Penrith NSW 2751, Australia, [14]Institute of Geographic Sciences and Natural Resources Research, Chinese Academy of Sciences, China, [15]Department of Mathematics, Imperial College, London, UK, [16]Biological Sciences Division,

Biogeosciences Discuss., doi:10.5194/bg-2016-377, 2016
Manuscript under review for journal Biogeosciences
Published: 16 September 2016

24 Pacific Northwest National Laboratory, Richland, Washington, USA,

25

26

27 **Running Title**: Land carbon storage dynamics

28

29 **Correspondence author**: Yiqi Luo

30 Email: yluo@ou.edu

31 **Key words** Carbon cycle, carbon sequestration, dynamic disequilibrium, model intercomparison,

32 terrestrial ecosystems, traceability analysis,

33 **Type of paper**: Primary Research Article

34

35

Biogeosciences Discuss., doi:10.5194/bg-2016-377, 2016
Manuscript under review for journal Biogeosciences
Published: 16 September 2016

Abstract Terrestrial ecosystems absorb roughly 30% of anthropogenic CO_2 emissions since preindustrial era, but it is unclear whether this carbon (C) sink will endure into the future. Despite extensive modeling, experimental, and observational studies, what fundamentally determines transient dynamics of terrestrial C storage under climate change is still not very clear. Here we develop a new framework for understanding transient dynamics of terrestrial C storage through mathematical analysis and numerical experiments. Our analysis indicates that the ultimate force driving ecosystem C storage change is the C storage capacity, which is jointly determined by ecosystem C input (e.g., net primary production, NPP) and residence time. Since both C input and residence time vary with time, the C storage capacity is time-dependent and acts as a moving attractor that actual C storage chases. The rate of change in C storage is proportional to the C storage potential, the difference between the current storage and the storage capacity. The C storage capacity represents instantaneous responses of the land C cycle to external forcing, whereas the C storage potential represents the internal capability of the land C cycle to influence the C change trajectory in the next time step. The influence happens through redistribution of net C pool changes in a network of pools with different residence times.

Moreover, this and our other studies have demonstrated that one matrix equation can exactly replicate simulations of most land C cycle models (i.e., physical emulators). As a result, simulation outputs of those models can be placed into a three-dimensional (3D) parameter space to measure their differences. The latter can be decomposed into traceable components to track the origins of model uncertainty. Moreover, the emulators make data assimilation computationally feasible so that both C flux- and pool-related datasets can be used to better constrain model predictions of land C sequestration. We also propose that the C storage potential be the targeted variable for research, market trading, and government negotiation for C credits.

Biogeosciences Discuss., doi:10.5194/bg-2016-377, 2016
Manuscript under review for journal Biogeosciences
Published: 16 September 2016

1 Introduction

Terrestrial ecosystems have been estimated to sequester approximately 30% of anthropogenic carbon (C) emission in the past three decades (Canadell et al., 2007). Cumulatively, land ecosystems have sequestered more than 160 Gt C from 1750 to 2015 (Le Quéré et al., 2015). Without land C sequestration, the atmospheric CO_2 concentration would have increased by additional 95 parts per million and result in more climate warming (Le Quéré et al., 2015). During one decade from 2005 to 2014, terrestrial ecosystems sequestrated 3±0.8 Gt C per year (Le Quéré et al., 2015), which would cost billion dollars if the equivalent amount of C was sequestrated using C capture and storage techniques (Smith et al., 2016). Thus, terrestrial ecosystems effectively mitigate climate change through natural processes with minimal cost. Whether this terrestrial C sequestration would endure into the future, however, is not clear, making the mitigation of climate change greatly uncertain. To predict future trajectories of C sequestration in the terrestrial ecosystems, it is essential to understand fundamental mechanisms that drive terrestrial C storage dynamics.

To predict future land C sequestration, the modeling community has developed many C cycle models. According to a review by Manzoni and Porporato (2009), approximately 250 biogeochemical models have been published over a time span of 80 years to describe carbon and nitrogen mineralization. The majority of those 250 models follow some mathematical formulations of ordinary differential equations. Moreover, many of those biogeochemical models incorporate more and more processes in an attempt to simulate C cycle processes as realistically as possible (Oleson et al., 2013). As a consequence, terrestrial C cycle models have become increasingly complicated and less tractable. Almost all model intercomparison projects (MIPs), including those involved in the last three IPCC assessments, indicate that C cycle models have

Biogeosciences Discuss., doi:10.5194/bg-2016-377, 2016
Manuscript under review for journal Biogeosciences
Published: 16 September 2016

consistently projected widely spread trajectories of land C sinks and also found to fit observations poorly (Todd-Brown et al., 2013; Luo et al., 2015). The lack of progress in uncertainty analysis urges us to understand mathematical foundation of those terrestrial C models so as to diagnose causes of model spreads and improve model predictive skills.

Meanwhile, many countries have made great investments on various observational and experimental networks (or platforms) in hope to quantify terrestrial C sequestration. For example, FLUXNET has been established about 20 years ago to quantify net ecosystem exchange (NEE) between the atmosphere and biosphere (Baldocchi et al., 2001). Orbiting Carbon Observatory 2 (OCO-2) satellite was launched in 2014 to quantify carbon dioxide concentrations and distributions in the atmosphere at high spatiotemporal resolution to constrain land surface C sequestration (Hammerling et al., 2012). Networks of global change experiments have been designed to uncover processes that regulate ecosystem C sequestration (Rustad et al., 2001; Luo et al., 2011; Fraser et al., 2013; Borer et al., 2014). Massive data has been generated from those observational systems and experimental networks. They offer an unprecedented opportunity for advancing our understanding of ecosystem processes and constraining model prediction of ecosystem C sequestration. Indeed, many of those networks were initiated with one goal to improve our predictive capability. Yet the massive data have been rarely integrated into earth system models to constrain their predictions. It is a grand challenge in our era to develop innovative approaches to integration of big data into complex models so as to improve prediction of future ecosystem C sequestration.

From a system perspective, ecosystem C sequestration occurs only when the terrestrial C cycle is in a transient state, under which C influx into one ecosystem is larger than C efflux from the ecosystem. Olson (1963) is probably among the first to examine organic matter storage at

Biogeosciences Discuss., doi:10.5194/bg-2016-377, 2016
Manuscript under review for journal Biogeosciences
Published: 16 September 2016

105 forest floors from the system perspective. His analysis approximated steady-state storage of
106 organic matter as a balance of litter producers and decomposers for different forest types.
107 However, climate change differentially influences different C cycle processes in ecosystems and
108 results in transient dynamics of terrestrial C storage (Luo and Weng, 2011). For example, rising
109 atmospheric CO_2 concentration primarily stimulates photosynthetic C uptake while climate
110 warming likely enhances decomposition. When ecosystem C uptake increases in a unidirectional
111 trend under elevated [CO_2], terrestrial C cycle is at disequilibrium, leading to net C storage. The
112 net gained C is first distributed to different pools, each of which has a different turnover rate (or
113 residence time) before C is eventually released back to the atmosphere via respiration.
114 Distribution of net C exchange to multiple pools with different residence times is an intrinsic
115 property of an ecosystem to gradually equalize C efflux with influx (i.e. internal recovery force
116 toward an attractor). In contrast, climate change that causes changes in C input and
117 decomposition is considered external forces that create disequilibrium through altering internal C
118 processes and pool sizes. The transient dynamics of terrestrial C cycle at disequilibrium is
119 maintained by interactions of internal processes and external forces (Luo and Weng, 2011).
120 Although the transient dynamics of terrestrial C storage have been conceptually discussed, we
121 still lack a quantitative formulation to estimate transient C storage dynamics in the terrestrial
122 ecosystems.
123 This paper was designed to address a question: what determines transient dynamics of C
124 storage in terrestrial ecosystems from a system perspective? We first reviewed the major
125 processes that most models have incorporated to simulate terrestrial C sequestration. The review
126 helps establish that terrestrial C cycle can be mathematically represented by a matrix equation.
127 We also described the Terrestrial ECOsystem (TECO) model with its numerical experiments in

Biogeosciences Discuss., doi:10.5194/bg-2016-377, 2016
Manuscript under review for journal Biogeosciences
Published: 16 September 2016

support of the mathematical analysis. We then presented results of mathematical analysis on determinants of the terrestrial C storage, direction and magnitude of C storage at a given time point, numerical experiments to illustrate climate impacts on terrestrial C storage. We carefully discussed assumptions of those terrestrial C cycle models as represented by the matrix equation, the validity of this analysis, and two new concepts introduced in this study, which are the C storage capacity and C storage potential. We also discussed the potential applications of this analysis to model uncertainty analysis and data-model integration. Moreover, we proposed that the C storage potential be a targeted variable for research, trading, and government negotiation for C credit.

2 Methods

2.1 Mathematical representation of terrestrial C cycle

This study was conducted mainly with mathematical analysis. We first established the basis of this analysis, which is that the majority of terrestrial C cycle models can be represented by a matrix equation.

Hundreds of models have been developed to simulate terrestrial C cycle (Manzoni and Porporato, 2009). All the models have to simulate processes of photosynthetic C input, C allocation and transformation, and respiratory C loss. It is well understood that photosynthesis is a primary pathway of C flow into land ecosystems. Photosynthetic C input is usually simulated according to carboxylation and electron transport rates (Farquhar et al., 1980). Ecosystem C influx varies with time and space mainly due to variations in leaf photosynthetic capacity, leaf area index of canopy, and a suite of environmental factors such as temperature, radiation, and relative humidity (or other water-related variables) (Potter et al., 1993; Sellers et al., 1996;

Biogeosciences Discuss., doi:10.5194/bg-2016-377, 2016
Manuscript under review for journal Biogeosciences
Published: 16 September 2016

151 Keenan et al., 2012; Walker et al., 2014).

152 Photosynthetically assimilated C is partly used for plant biomass growth and partly
153 released back into the atmosphere through plant respiration. Plant biomass in leaves and fine
154 roots usually lives for several months up to a few years before death, while woody tissues may
155 persist for hundreds of years in forests. Dead plant materials are transferred to litter pools and
156 decomposed by microorganisms to be partially released through heterotrophic respiration and
157 partially stabilized to form soil organic matter (SOM). SOM can store C in the soil for hundreds
158 or thousands of years before it is broken down to CO_2 through microbial respiration (Luo and
159 Zhou, 2006). This series of C cycle processes has been represented in most ecosystem models
160 with multiple pools linked by C transfers among them (Jenkinson et al., 1987; Parton et al., 1987;
161 1988; 1993), including those embedded in earth system models (Ciais et al., 2013).

162 The majority of the published 250 terrestrial C cycle models use ordinary differential
163 equations to describe C transformation processes among multiple plant, litter, and soil pools
164 (Manzoni and Porporato, 2009). Those ordinary differential equations can be summarized into a
165 matrix formula (Luo et al., 2003; Luo and Weng, 2011; Luo et al., 2015; 2016; Sierra and Müller
166 2015) as:

167 $$X'(t) = Bu(t) - A\xi(t)KX(t) \quad (1)$$

168 where $X'(t)$ is a vector of net C pool changes at time t, $X(t)$ is a vector of pool sizes, B is a vector
169 of partitioning coefficients from C input to each of the pools, $u(t)$ is C input rate, A is a matrix of
170 transfer coefficients (or microbial C use efficiency) to quantify C movement along the pathways,
171 K is a diagonal matrix of exit rates (mortality for plant pools and decomposition coefficients of
172 litter and soil pools) from donor pools and $\xi(t)$ is a diagonal matrix of environmental scalars to
173 represent responses of C cycle to changes in temperature, moisture, nutrients, litter quality, and

Biogeosciences Discuss., doi:10.5194/bg-2016-377, 2016
Manuscript under review for journal Biogeosciences
Published: 16 September 2016

soil texture. In eq. 1, all the off-diagonal a_{ji} values are negative. The equation describes net C pool change, $X'(t)$, as a result of C input, $u(t)$, distributed to different plant pools via partitioning coefficients, B, minus C loss through C transformation matrix, $A\xi(t)K$, among individual pools, $X(t)$. Elements in vector B, matrices A and K could vary with many factors, such as vegetation types, soil textual, microbial attributes, and litter chemistry. For example, vegetation succession may influence elements in vector B, matrices A and K in addition to C input, $u(t)$, and forcing that affects C dynamics through environmental scalars, $\xi(t)$.

After synthesis of all the possible soil C cycle models based on six principles (mass balance, substrate dependence of decomposition, heterogeneity of decay rates, internal transformations of organic matter, environmental variability effects, and substrate interactions), Sierra and Müller (2015) concluded that this form of matrix equation such as eq. 1 represents the majority of terrestrial C cycle models. Similarly, Manzoni and Porporato (2009) concluded their review of 250 models that the majority of them use ordinary differential equations, which can be summarized by eq. 1, to describe land C cycle. Our mathematical analysis in this study used matrix operations of eq. 1 to reveal determinants of transient dynamics of terrestrial C cycle, including direction and rate of C storage changes, in response to climate change. We examined assumptions underlying this equation and the validity of our analysis in the Discussion section.

2.2 Model and its numerical experiments

We conducted numerical experiments to support the mathematical analysis and thus help understand the characteristics of terrestrial C storage dynamics using the Terrestrial ECOsystem (TECO) model. TECO has five major components: canopy photosynthesis, soil water dynamics, plant growth, litter and soil carbon decomposition and transformation, and nitrogen dynamics as

Biogeosciences Discuss., doi:10.5194/bg-2016-377, 2016
Manuscript under review for journal Biogeosciences
Published: 16 September 2016

described in detail by Weng and Luo (2008) and Shi et al. (2016). Canopy photosynthesis is referred from a two-leaf (sunlit and shaded) model developed by Wang and Leuning (1998). This submodel simulates canopy conductance, photosynthesis, and partitioning of available energy. The model combines the leaf photosynthesis model developed by Farquhar et al. (1980) and a stomatal conductance model (Harley et al., 1992). In the soil water dynamic submodel, soil is divided into 10 layers. The surface layer is 10 cm deep and the other 9 layers are 20 cm deep. Soil water content (SWC) in each layer results from the mass balance between water influx and efflux. The plant growth submodel simulates C allocation and phenology. Allocation of C among three plant pools, which are leaf, fine root, and wood, depends on their growth rates (Fig. 1a). Phenology dynamics is related to leaf onset, which is triggered by growing degree days, and leaf senescence, which is determined by temperature and soil moisture. The C transformation submodel estimates carbon transfer from plants to two litter pools and three soil pools (Fig. 1a). The nitrogen (N) submodel is fully coupled with C processes with one additional mineral N pool. Nitrogen is absorbed by plants from mineral soil and then partitioned among leaf, woody tissues and fine roots. Nitrogen in plant detritus is transferred among different ecosystem pools (i.e. litter, coarse wood debris, fast, slow and passive SOM) (Shi et al., 2016). The model is driven by climate data, which included air and soil temperature, vapor-pressure deficit, relative humidity, incident photosynthetically active radiation, and precipitation at hourly steps.

We first calibrated TECO with eddy flux data collected at Harvard Forest from 2006-2009. The calibrated model was spun up to the equilibrium state in pre-industrial environmental conditions by recycling a 10-year climate forcing (1850-1859). Then the model was used to simulate C dynamics from year 1850 to 2100 with the historical forcing scenario for 1850-2005 and RCP8.5 scenario for 2006-2100 as in the Community Land Model 4.5 (Oleson et al., 2013)

Biogeosciences Discuss., doi:10.5194/bg-2016-377, 2016
Manuscript under review for journal Biogeosciences
Published: 16 September 2016

220 in the grid cell where Harvard Forest is located.

221 To support the mathematical analysis using eq. 1, we first verified that eq. 1 can exactly
222 represent TECO model simulations. We first identified those variables in each of the C balance
223 equations in the TECO model that are corresponding to elements in matrices A, $\xi(t)$, and K, and
224 vectors $X(t)$, and B together with variable $u(t)$ in eq. 1. Then we ran the TECO model to
225 generate outputs of all those variables at each time step, which were consequently organized into
226 matrices A, $\xi(t)$, and K, and vectors $X(t)$ and B, and variable $u(t)$. Those matrices, vectors, and
227 variable were entered to matrix calculation to compute $X'(t)$ using eq. 1. The sum of elements in
228 calculated $X'(t)$ is a 100% match with simulated net ecosystem production (NEP) with the
229 TECO model (Fig. 1b).

230 Once eq. 1 was verified to exactly replicate TECO simulations, we use TECO to generate
231 numerical experiments to support the mathematical analysis on the transient dynamics of
232 terrestrial C storage. To analyze the seasonal patterns of C storage dynamics, we averaged 10
233 series of three-year seasonal dynamics from 1851-1880. Then we used a 7-day moving window
234 to further smooth the data.

235

236 **3. Results**

237

238 **3.1 Determinants of C storage dynamics**

239 The transient dynamics of terrestrial carbon storage are determined by two components: the C
240 storage capacity and the C storage potential. The two components of C storage dynamics can be
241 mathematically derived from multiplying both sides of eq. 1 by $(A\xi(t)K)^{-1}$ as:

242 $$X(t) = (A\xi(t)K)^{-1}Bu(t) - (A\xi(t)K)^{-1}X'(t) \quad (2)$$

Biogeosciences Discuss., doi:10.5194/bg-2016-377, 2016
Manuscript under review for journal Biogeosciences
Published: 16 September 2016

The first term on the left side of eq. 2 is the C storage capacity and the second term is the C storage potential. Fig. 2a shows time courses of C storage and its capacity over one year for the leaf pool of Harvard Forest.

In eq. 2, we name the term $(A\xi(t)K)^{-1}$ the chasing time, $\tau_{ch}(t)$, as:

$$\tau_{ch}(t) = (A\xi(t)K)^{-1} \quad (3)$$

$\tau_{ch}(t)$ is a matrix of C residence times through the network of individual pools each with different capacities as measured by their residence times and fractions of received C connected by pathways of C transfer. Analogous to the fundamental matrix measuring life expectancies in demographic models (Caswell, 2000), the matrix, $\tau_{ch}(t)$, here measures expected residence time of a C atom in pool *i* when it has entered from pool *j*. We call this matrix the fundamental matrix of chasing times to represent the time scale at which the net C pool change, $X'(t)$, is redistributed in the network. Meanwhile, the residence time of individual pools in network can be estimated by multiplying the fundamental matrix of chasing times, $(A\xi(t)K)^{-1}$, by a vector of partitioning coefficients, *B* as:

$$\tau_E(t) = (A\xi(t)K)^{-1}B \quad (4)$$

Ecosystem residence time is the sum of the residence time of all individual pools in network,

Thus, the C storage capacity can be defined by:

$$X_c(t) = (A\xi(t)K)^{-1}Bu(t) \quad (5a)$$

Or it can be estimated from input C, $u(t)$, and residence time, $\tau_E(t)$, as:

$$X_C(t) = \tau_E(t)u(t) \quad (5b)$$

As C input (e.g., Gross or Net Primary Productions, GPP or NPP) and residence times vary with time, the C storage capacity varies with time. It represents instantaneous responses of the terrestrial C cycle to the external forcing. The modeled C storage capacity in the leaf pool (Fig.

Biogeosciences Discuss., doi:10.5194/bg-2016-377, 2016
Manuscript under review for journal Biogeosciences
Published: 16 September 2016

2a), for example, increases in spring, reaches the peak at summer, declines in autumn, and becomes minimal in winter largely due to strong seasonal changes in C input (Fig. 2b). Note that either GPP or NPP can be used as C input for analysis of transient C dynamics. Estimated residence times, however, are smaller with GPP as C input than those with NPP as input. In this paper, we mostly used NPP as C input as that fraction of C is distributed among pools.

The C storage potential at time *t*, $X_p(t)$, can be mathematically described as:

$$X_p(t) = (A\xi(t)K)^{-1}X'(t) \quad (6a)$$

Or it can be estimated from net C pool change, $X'(t)$, and chasing time, $\tau_{ch}(t)$ as:

$$X_p(t) = \tau_{ch}(t)X'(t) \quad (6b)$$

Eqs. 6a and 6b suggest that the C storage potential represents re-distribution of net C pool change, $X'(t)$, of individual pools through a network of pools with different residence times as connected by C transfers from one pool to the others through all the pathways. As time evolves, the net C pool change, $X'(t)$, is redistributed again and again through the network of pools. The network of redistribution of next C pool change, thus, represents the potential of an ecosystem to store additional C when it is positive and lose C when it is negative. The C storage potential can also be estimated from the difference between the C storage capacity and the C storage itself at time *t* as:

$$X_p(t) = X_c(t) - X(t) \quad (6c)$$

The C storage potential in the leaf pool, for example, is about zero in winter and early spring when the C storage capacity is very close to the storage itself (Fig. 2a). The C storage potential is positive when the capacity is larger than the storage itself from late spring to summer and early fall. As the storage capacity decreases to the point when the storage equals the capacity on the 265th day of year (DOY), the C storage potential is zero. After that day, the C storage potential

Biogeosciences Discuss., doi:10.5194/bg-2016-377, 2016
Manuscript under review for journal Biogeosciences
Published: 16 September 2016

289 becomes negative.

290 Dynamics of ecosystem C storage, $X(t)$, can be characterized by three parameters: C
291 influx, $u(t)$, residence times, $\tau_E(t)$, and the C storage potential $X_p(t)$ as:

292 $$X(t) = \tau_E(t)u(t) - X_p(t) \quad (7)$$

293 Eq. 7 represents a three-dimensional (3D) parameter space within which model simulation
294 outputs can be placed to measure how and how much they diverge.

295 Note that sums of elements in vectors $X(t)$, $X_c(t)$, $X_p(t)$, $X'(t)$, and $\tau_E(t)$ are
296 corresponding, respectively, to the whole ecosystem C stock, ecosystem C storage capacity,
297 ecosystem C storage potential, net ecosystem production (NEP), and ecosystem residence time.
298 In this paper, we do not use a separate set of symbols to represent those sums rather than express
299 them wherever necessary.

300

301 **3.2 Direction and rate of C storage change at a given time**

302 Like studying any moving object, quantifying dynamics of land C storage needs to determine
303 both the direction and the rate of its change at a given time. To determine the direction and rate
304 of C storage change, we re-arranged eq. 2 to be:

305 $$\tau_{ch}X'(t) = X_c(t) - X(t) = X_p(t) \quad (8a)$$

306 or re-arranging eq. 6a leads to:

307 $$X'(t) = A\xi(t)KX_p(t) \quad (8b)$$

308 As all the elements in τ_{ch} are positive, the sign of $X'(t)$ is the same as for $X_p(t)$. That means
309 $X'(t)$ increases when $X_c(t) > X(t)$, does not change when $X_c(t) = X(t)$, and decreases when
310 $X_c(t) < X(t)$ at the ecosystem scale. Thus, the C storage capacity, $X_c(t)$, is an attractor and

Biogeosciences Discuss., doi:10.5194/bg-2016-377, 2016
Manuscript under review for journal Biogeosciences
Published: 16 September 2016

311 hence determines the direction toward which the C storage, $X(t)$, chases at any given time point.
312 The rate of C storage change, $X'(t)$, is proportional to $X_p(t)$ and also regulated by τ_{ch}.

313 When we study C cycle dynamics, we are not only interested in understanding dynamics
314 of a whole ecosystem but also individual pools. Eq. 8a can be used to derive equations to
315 describe C storage change for an i[th] pool as:

316 $$\sum_{j=1}^{n} f_{ij}\,\tau_i\,x'_j(t) = \sum_{j=1}^{n} f_{ij}\,\tau_i b_j u(t) - x_i(t) = x_{p,i}(t) \qquad (9a)$$

317 where n is the number of pools in a C cycle model, f_{ij} is a fraction of C transferred from pool j
318 to i through all the pathways, τ_i measure residence times of individual pools in isolation, x'_j is
319 the net C change in the j[th] pool, b_j is a partitioning coefficient of C input to the j[th] pool, $x_i(t)$ is
320 the C storage in the i[th] pool, and $x_{p,i}(t)$ is the C storage potential in the i[th] pool. Eq. 9a means
321 that the C storage potential of each pool at time t, $x_{p,i}(t)$, is the sum of all the individual net C
322 pool change, x'_j, multiplied by corresponding residence time spent in pool i coming from pool j.
323 Through re-arrangement, eq. 9a can be solved for each individual pool net C change as a
324 function of C storage potential of all the pools as:

325 $$x'_i(t) = \frac{x_{c,i,u}(t) - x_{c,i,p}(t) - x_i(t)}{f_{ii}\tau_i} \qquad (9b)$$

326 where $x_{c,i,u}(t) = \sum_{j=1}^{n} f_{ij}\,\tau_i b_j u(t)$ for the maximal amount of C that can transfer from C input
327 to the i[th] pool. $x_{c,i,p}(t) = \sum_{j=1,j\neq i}^{n} f_{ij}\,\tau_i x'_j(t)$ for the maximal amount of C that can transfer from
328 all the other pools to the i[th] pool. $f_{ii} = 1$ for all the pools if there is no feedback of C among soil
329 pools. $f_{ii} < 1$ when there are feedbacks of C among soil pools.

330 As plant pools get C only from photosynthetic C input, $u(t)$, but not from other pools,
331 the direction and rate of C storage change in the i[th] plant pool is determined by:

Biogeosciences Discuss., doi:10.5194/bg-2016-377, 2016
Manuscript under review for journal Biogeosciences
Published: 16 September 2016

$$\begin{cases} x'_i(t) = \frac{x_{c,i}(t) - x_i(t)}{\tau_i} = \frac{X_{p,i}(t)}{\tau_i} \\ x_{c,i}(t) = b_i u(t) \tau_i \end{cases} \quad \text{for i = 1, 2, 3} \qquad (10)$$

The C storage capacity of plant pools equals the product of plant C input, $u(t)$ (i.e., net primary production, NPP), partitioning coefficient, b_i, and residence time, τ_i, of its own pool (Fig. 2b-d). Thus, the C storage capacities of the leaf, root, and wood pools are high in summer and low in winter. Plant C storage, $x_i(t)$, still chases the storage capacity, $x_{c,i}(t)$, of its own pool at a rate that is proportional to $X_{p,i}(t)$. For the leaf pool, the C storage, $x_1(t)$, increases when $x_{c,1}(t) > x_1(t)$ (or $x_{p,1}(t)>0$) from late spring until early fall on the 265th day of year (DOY) and then decreases when $x_{c,1}(t) < x_1(t)$ (or $x_{p,1}(t)<0$) from DOY of 265 until 326 during fall (Fig. 2a).

However, the direction of C storage change in litter and soil pools are no longer solely determined by the storage capacity, $x_{c,i}(t)$, of their own pools or at a rate that is proportional to $X_{p,i}(t)$. The C storage capacity of one litter or soil pool has two components. One component, $x_{c,i,u}(t)$ is set by the amount of plant C input, $u(t)$, going through all the possible pathways, $f_{ij}b_j$, multiplied by residence time, τ_i, of its own pool. The second component measures the C exchange of one litter or soil pool with other pools according to net C pool change, $x'_j(t)$, through pathways, $f_{ij}, j \neq i$, weighed by residence time, τ_i, of its own pool. For example, C input to the litter pool is a combination of C transfer from C input through the leaf, root, and wood pools (Fig. 3c, 3d, and 3e) and C transfer due to the net C pool changes in the leaf, root, and wood pools (Fig. 3f, 3g, and 3h). Thus the first capacity component of the litter pool to store C is the sum of three products of NPP, C partitioning coefficient, and network residence time, respectively, through the leaf, root, and wood pools (Fig. 3c, 3d, and 3e). The second capacity component is the sum of other three products of C transfer coefficient along all the possible pathways, network residence time, and net C pool changes, respectively, in the leaf, root, and

Biogeosciences Discuss., doi:10.5194/bg-2016-377, 2016
Manuscript under review for journal Biogeosciences
Published: 16 September 2016

wood pools (Fig. 3f, 3g, and 3h). Thus, C storage in the i^{th} pool, $x_i(t)$, chases an attractor, $(\sum_{j=1}^{n} f_{ij}\, b_j u(t) - \sum_{j=1, j\neq i}^{n} f_{ij}\, \tau_i x'_j(t))\tau_i$, for litter and soil pools (Fig. 4).

In summary, due to the network of C transfer, C storage in litter and soil pools does not chase the C storage capacities of their own pools in a multiple C pool model (Fig. 4). The capacities for individual litter and soil pools measure the amounts of C that is transferred from photosynthetic C input through plant pools to be stored in those pools. However, those litter and soil pools also exchange C with other pools according to transfer coefficients along pathways of C movement multiplying net C pool change in those pools. Integration of the C input and C exchanges together still set as a moving attractor toward which individual pool C storage approaches (Fig. 4).

3.3 C storage dynamics under climate change

In response to a climate change scenario that combines historical change and simulated RCP8.5 in the TECO experiment, the modeled ecosystem C storage capacity (the sum of all elements in vector $X_c(t)$) at Harvard Forest increases from 27 kg C m^{-2} in 1850 to approximately 38 kg C m^{-2} in 2100 with strong interannual variability (Fig. 5a). The increasing capacity results from a combination of a nearly 44% increase in NPP with a ~2% decrease in ecosystem residence times (the sum of all elements in vector $\tau_E(t)$) during that period (Fig. 5b). The strong interannual variability in the modeled capacity is attributable to the variability in NPP and residence times, both of which directly respond to instantaneous variations in environmental factors. In comparison, the ecosystem C storage (the sum of all elements in vector $X(t)$) itself gradually increases, lagging behind the capacity, with much dampened interannual variability (Fig. 5a). The dampened interannual variability is due to smoothing effects of pools with various residence

Biogeosciences Discuss., doi:10.5194/bg-2016-377, 2016
Manuscript under review for journal Biogeosciences
Published: 16 September 2016

377 times. In response to climate change scenario RCP8.5, the ecosystem C storage potential (the
378 sum of all elements in vector $X_p(t)$) in the Harvard Forest ecosystem increases from zero at
379 1980 to 3.5 kg C m^{-2} in 2100 with strong fluctuation over years (Fig. 5a). Over seasons, the
380 potential is high during the summer and low in winter, similarly with the seasonal cycle of the C
381 storage capacity.

382 Since chasing time, τ_{ch}, is a matrix and net C pool change, $X'(t)$, is a vector, eq. 6a or 6b
383 (i.e., the C storage potential) can not be analytically separated into the chasing time and net C
384 pool change as can the capacity into C input and residence time in eq. 5a or 5b for traceability
385 analysis. The relationships among the three quantities can be explored by regression analysis.
386 The ecosystem C storage potential fluctuates in a similar phase with NEP from 1850 to 2100
387 (Fig. 5c). Consequently, the C storage potential is well correlated with NEP at the whole
388 ecosystem scale (Fig. 5d). The slope of the regression line is a statistical representation of
389 ecosystem chasing time. In this study, we find that r^2 of the relationship between the storage
390 potential and NEP is 0.79. The regression slope is 28.1 years in comparison with the ecosystem
391 residence time of approximately 22 years (Fig. 5b).

392 The capacity and storage itself of individual pools display similar long-term trends and
393 interannual variability to those for the total ecosystem C storage dynamics (Fig. 6). Noticeably,
394 the deviation of the C storage from the capacity, which is the C storage potential, is much larger
395 for pools with long residence times than those with short residence times. For individual pools,
396 the potential is nearly zero for those fast turnover pools and becomes very large for those pools
397 with long residence time (Fig. 6).

398 For individual plant pools, eq. 10 describes the dependence of the C storage potential,
399 $x_{p,i}(t)$, on the pool-specific residence time, τ_i, i = 1, 2, and 3, and net C pool change of their

Biogeosciences Discuss., doi:10.5194/bg-2016-377, 2016
Manuscript under review for journal Biogeosciences
Published: 16 September 2016

own pools, $x'_i(t), i$ = 1, 2, and 3. Thus, one value of $x_{p,i}(t)$ is exactly corresponding to one value of $x'_i(t)$ at slope of τ_i, leading to the correlation coefficient in Fig. 7 being 1.00 for leaf, root, and wood pools. For a litter or soil pool, however, the C storage potential is not solely dependent on the residence time and net C pool change of its own pool but influenced by several other pools. Thus, the potential of one litter or soil pool is correlated with net C pool changes of several pools with different regression slopes (Fig. 7).

4 Discussion

4.1 Assumptions of the C cycle models and validity of this analysis

This analysis is built upon eq. 1, which represents the majority of terrestrial C cycle models developed in the past decades (Manzoni and Porporato, 2009; Sierra and Müller, 2015). Those models have several assumptions, which may influence the validity of this analysis. First, those models assume that donor pools control C transfers among pools and decomposition follows 1st-order decay functions (Assumption 1). This assumption is built upon observations from litter and SOC decomposition. Analysis of data from nearly 300 studies of litter decomposition (Zhang et al., 2008), about 500 studies of soil incubation (Xu et al., 2016), more than 100 studies of forest succession (Yang et al., 2011), and restoration (Matamala et al., 2008) almost all suggest that the 1st-order decay function captures macroscopic patterns of land C dynamics. Even so, its biological, chemical and physical underpinnings need more study (Luo et al., 2016). This assumption has recently been challenged by a notion that microbes are actively involved in decomposition processes. To describe the active roles of microbes in organic C decomposition, a suite of nonlinear microbial models has been proposed using Michaelis-Menten or reverse Michaelis-Menten equations (Allison et al., 2010; Wieder et al., 2013). Those

Biogeosciences Discuss., doi:10.5194/bg-2016-377, 2016
Manuscript under review for journal Biogeosciences
Published: 16 September 2016

423 nonlinear models exhibit unique behaviors of modeled systems, such as damped oscillatory
424 responses of soil C dynamics to small perturbations and insensitivity of the equilibrium pool
425 sizes of litter or soil carbon to inputs (Li et al., 2014; Wang et al., 2014; 2016). Oscillations have
426 been documented for single enzymes at timescales between 10^{-4} to 10 seconds (English et al.,
427 2006; Goldbeter, 2013; Xie, 2013). Over longer timescales with mixtures of large diversity of
428 enzyme-substrate complexes in soil, oscillations may be likely averaged out so that the 1st order
429 decay functions may well approximate these average dynamics of organic matter decomposition
430 (Sierra and Müller, 2015).

431 Second, those models all assume that multiple pools can adequately approximate
432 transformation, decomposition, and stabilization of SOC in the real world (Assumption 2). The
433 classic SOC model, CENTURY, uses three conceptual pools, active, slow, and passive SOC, to
434 represent SOC dynamics (Parton et al., 1987). Several models define pools that are
435 corresponding to measurable SOC fractions to match experimental observation with modeling
436 analysis (Smith et al., 2002; Stewart et al., 2008). Carbon transformation in soil over time has
437 also been described by a partial differential function of SOM quality (Bosatta and Ågren, 1991;
438 Ågren and Bosatta, 1996). The latter quality model describes the external inputs of C with
439 certain quality, C loss due to decomposition, and the internal transformations of the quality of
440 soil organic matter. It has been shown that multi-pool models can approximate the partial
441 differential function or continuous quality model as the number of pools increases (Bolker et al.,
442 1998; Sierra and Müller, 2015).

443 Assumption 3 is on partitioning coefficients of C input (i.e., elements in vector B) and C
444 transformation among plant, litter, and soil pools (i.e., elements in the matrix, $A\xi(t)K$). Some of
445 the terrestrial C cycle models assume that elements in vector B, and matrices A and K are

Biogeosciences Discuss., doi:10.5194/bg-2016-377, 2016
Manuscript under review for journal Biogeosciences
Published: 16 September 2016

446 constants. All the factors or processes that vary with time are represented in the diagonal matrix
447 $\xi(t)$. In the real world, C transformation are influenced by environmental variables (e.g.,
448 temperature, moisture, oxygen, N, phosphorus, and acidity varying with soil profile, space, and
449 time), litter quality (e.g., lignin, cellulose, N, or their relative content), organomineral properties
450 of SOC (e.g., complex chemical compounds, aggregation, physiochemical binding and
451 protection, reactions with inorganic, reactive surfaces, and sorption), and microbial attributes
452 (e.g., community structure, functionality, priming, acclimation, and other physiological
453 adjustments) (Luo et al., 2016). It is not practical to incorporate all of those factors and processes
454 into one model. Only a subset of them is explicitly expressed while the majority is implicitly
455 embedded in the C cycle models. Empirical studies have suggested that temperature, moisture,
456 litter quality, and soil texture are primary factors that control C transformation processes of
457 decomposition and stabilization (Burke et al., 1989; Adair et al., 2008; Zhang et al., 2008; Xu et
458 al., 2012; Wang et al., 2013). Nitrogen influences C cycle processes mainly through changes in
459 photosynthetic C input, C partitioning, and decomposition. It is yet to identify how other major
460 factors and processes, such as microbial activities and organomineral protection, regulate C
461 transformation.

462 Assumption 4 is that terrestrial C cycle models use different response functions (i.e.,
463 different $\xi(t)$ in eq. 1) to represent C cycle responses to external variables. As temperature
464 modifies almost all processes in the C cycle, different formulations, including exponential,
465 Arrhenius, and optimal response functions, have been used to describe C cycle responses to
466 temperature changes in different models (Lloyd and Taylor, 1994; Jones et al., 2005; Sierra and
467 Müller, 2015). Different response functions are used to connect C cycle processes with moisture,
468 nutrient availability, soil clay content, litter quality, and other factors. Different formulations of

Biogeosciences Discuss., doi:10.5194/bg-2016-377, 2016
Manuscript under review for journal Biogeosciences
Published: 16 September 2016

469 response functions may result in substantially different model projections (Exbrayat et al., 2013)
470 but unlikely change basic dynamics of the model behaviors.

471 Assumption 5 is that disturbance events are represented in models in different ways
472 (Grosse et al., 2011; West et al., 2011; Goetz et al., 2012; Hicke et al., 2012). Fire, extreme
473 drought, insect outbreaks, land management, and land cover and land use change influence
474 terrestrial C dynamics via 1) altering rate processes, for example, gross primary productivity
475 (GPP), growth, tree mortality, or heterotrophic respiration; 2) modifying microclimatic
476 environments; 3) transferring C from one pool to another (e.g., from live to dead pools during
477 storms or release to the atmosphere with fire) (Kloster et al., 2010; Thonicke et al., 2010; Luo
478 and Weng, 2011; Prentice et al., 2011; Weng et al., 2012). Many disturbance events are
479 incorporated into terrestrial C cycle models without changing the basic formulation (i.e., eq. 1)
480 (Weng et al., 2012).

481 The sixth assumption that those models make is that the lateral C fluxes through erosion
482 or local C drainage is negligible so that eq (1) can approximate terrestrial C cycle over space. If
483 soil erosion is substantial enough to be modeled with horizontal movement of C, a third
484 dimension should be added in addition to two-dimensional transfers in classic models.

485 Our analysis on transient dynamics of terrestrial C cycle is valid unless some of the
486 assumptions are violated. Assumption 1 on the 1^{st}-order decay function of decomposition
487 appears to be supported by thousands of datasets. It is a burden on microbiologists to identify
488 empirical evidence to support the nonlinear microbial models. Assumption 2 may not affect the
489 validity of our analysis no matter how C pools are divided in the ecosystems. Our analysis in this
490 study is applicable no matter whether elements are time-varying or constant in vector B and
491 matrices A and K as in assumption 3. Neither assumption 4 nor 5 would affect the analysis in this

Biogeosciences Discuss., doi:10.5194/bg-2016-377, 2016
Manuscript under review for journal Biogeosciences
Published: 16 September 2016

492 study. The environmental scalar, $\xi(t)$, as related to assumption 4 can be any forms in the derived
493 equations (e.g., eq. 2). Disturbances of fire, land use, and extreme drought change rate processes
494 but do not alter the basic formulation of eq. 1. If soil erosion and lateral transportation of C
495 become a major research objective, Eq. (1) can no longer be analyzed to understand the
496 mathematical foundation underlying transient dynamics of terrestrial C cycle.
497
498 **4.2 Carbon storage capacity**
499 One of the two components this analysis introduces to understand transient dynamics of
500 terrestrial C storage is the C storage capacity (Eq. 2). Olson (1963) is probably among the first
501 who systematically analyzed C storage dynamics at forest floor as functions of litter production
502 and decomposition. He collected data of annual litter production and approximately steady-state
503 organic C storage at forest floor, from which decomposition rates were estimated for a variety of
504 ecosystems from Ghana in the tropics to alpine forests in California. Using the relationships
505 among litter production, decomposition, and C storage, Olson (1963) explored several issues,
506 such as decay without input, accumulation with continuous or discrete annual litter fall, and
507 adjustments in production and decay parameters during forest succession. His analysis
508 approximated the steady-state C storage as the C input times the inverse of decomposition (i.e.,
509 residence time). The steady-state C storage is also considered the maximal amount of C that a
510 forest can store.
511 This study is not only built upon Olson's analysis but also expands it at least in two
512 aspects. First, we similarly define the C storage capacity (i.e., eqs. 5a and 5b). Those equations
513 can be applied to a whole ecosystem with multiple C pools while Olson's analysis is for one C
514 pool. Second, Olson (1963) treated the C input and decomposition rate as yearly constants at a

Biogeosciences Discuss., doi:10.5194/bg-2016-377, 2016
Manuscript under review for journal Biogeosciences
Published: 16 September 2016

given location even though they varied with locations. This study considers both C input and rate of decomposition being time dependent. A dynamical system with its input and parameters being time dependent mathematically becomes a nonautonomous system (Kloeden and Rasmussen, 2011). As terrestrial C cycle under climate change is transient, we need to treat it a nonautonomous system to better understand the properties of transient dynamics. Olson (1963) approximated the non-autonomous system at the yearly time scale without climate change so as to effectively understand properties of the steady-state C storage at the forest floor. In comparison, eqs. 5a and b are not only more general but also essential for understanding transient dynamics of the terrestrial C cycle in response to climate change.

Under the transient dynamics, the C storage capacity as defined by eqs 5a and b still sets the maximal amount of C that one ecosystem can store at time *t*. This capacity represents instantaneous responses of ecosystem C cycle to external forcing via changes in both C input and residence time, and thus varies within one day, over seasons of a year, and interannually over longer time scales as forcings vary. The variation of the C storage capacity can result from cyclic environmental changes (e.g., dial and seasonal changes), directional climate change (e.g., rising atmospheric CO_2, nitrogen deposition, altered precipitation, and warming), disturbance events, disturbance regime shifts, and changing vegetation dynamics (Luo and Weng, 2011). As the capacity sets the maximal amount of C storage (Fig. 2a), it is a moving attractor toward which the current C storage chases. When the capacity is larger than the C storage itself, C storage increases. Otherwise, the C storage decreases.

4.3 Carbon storage potential

The C storage potential represents the internal capability to equilibrate the current C

Biogeosciences Discuss., doi:10.5194/bg-2016-377, 2016
Manuscript under review for journal Biogeosciences
Published: 16 September 2016

538 storage with the capacity. Bogeochemically, the C storage potential represents re-distribution of
539 net C pool change, $X'(t)$, of individual pools through a network of pools with different residence
540 times as connected by C transfers from one pool to the others through all the pathways. The
541 potential is conceptually equivalent to the magnitude of disequilibrium as discussed by Luo and
542 Weng (2011).

543 The C storage potential measures the amount of additional C that one ecosystem can
544 store. Thus it can be used as a targeted quantity for C cycle research, C trading, and C credit in
545 government negotiation. In many fields of research, there are clearly targeted quantities on which
546 research would be focused. For example, crop science primarily focuses on crop yield although
547 environmental consequences of increasing crop yield have to be quantified. Gross domestic
548 product (GDP) is the targeted indicator that a country manages their economy. Although C cycle
549 has become a major research topic, has markets for trading, and is managed by governments, no
550 consensus has been established on the targeted quantity that our study should focus on.

551 Extensive studies have been done to quantify terrestrial C sequestration. The most
552 commonly estimated quantities for C sequestration include net ecosystem exchange (NEE), C
553 stocks in ecosystems (i.e., plant biomass and SOC) and their changes (Baldocchi et al., 2001; Pan
554 et al., 2013). This study, for the first time, offers the theoretical basis to estimate the terrestrial C
555 storage potential in at least two approaches: (1) the product of chasing time and net C pool
556 change with eqs. 6a and 6b; and (2) the difference between the C storage capacity and the C
557 storage itself with eqs. 6c. Since the time-varying C storage capacity is fully defined by
558 residence time and C input at any given time, C storage potential can be estimated from three
559 quantities: C input, residence time, and C storage.

560 To effectively quantify the C storage potential in terrestrial ecosystems, we need various

Biogeosciences Discuss., doi:10.5194/bg-2016-377, 2016
Manuscript under review for journal Biogeosciences
Published: 16 September 2016

data sets from experimental and observatory studies to be first assimilated into models. For example, data from Harvard Forest were first used to constrain the TECO model. The constrained model was used to explore changes in ecosystem C storage in response to climate change scenario, RCP8.5. That scenario primarily stimulated NPP, which increased from 1.06 to 1.8 kg C m^{-2} yr^{-1} in the Harvard Forest (Fig. 5b). Although climate warming decreased residence time in the Harvard Forest, the substantial increases in NPP resulted in increases in the C storage potential over time.

4.4 Novel approaches to model evaluation and improvement

Our analysis of transient C cycle dynamics offers new approaches to understand, evaluate, diagnose, and improve land C cycle models. We have demonstrated that many global land C cycle models can be exactly represented by the matrix equation (Eqs. 1 and 2) (i.e., physical emulators). As a consequence, outputs of all those models can be placed into a three dimensional (3D) space (Eq. 7) to measure their differences. In addition, components of land C cycle models are simulated in a mutually independent fashion so that modeled C storage can be decomposed into traceable components for traceability analysis. Moreover, the physical emulators computationally enable data assimilation to constrain complex models.

Physical Emulators of land C cycle models We have developed matrix representations (i.e., physical emulators) of CABLE, LPJ-GUESS, CLM3.5, CLM 4.0, CLM4.5, BEPS, and TECO (Xia et al., 2013; Hararuk et al., 2014; Ahlström et al., 2015; Chen et al., 2015). The emulators can exactly replicate simulations of C pools and fluxes with their original models when driven by a limited set of inputs from the full model (GPP, soil temperature, and soil moisture) (Fig. 1b and 1c). The emulators make complex models analytically clear and,

Biogeosciences Discuss., doi:10.5194/bg-2016-377, 2016
Manuscript under review for journal Biogeosciences
Published: 16 September 2016

584 therefore, give us a way to understand the effects of forcing, model structures, and parameters on
585 modeled ecosystem processes. They greatly simplify the task of understanding the dynamics of
586 submodels and interactions between them. The emulators allow us analyze model results in the
587 3D parameter space and the traceability framework.

588 *Parameter space of C cycle dynamics* Eq. 7 indicates that transient dynamics of modeled
589 C storage are determined by three parameters: C input, residence time, and C storage potential.
590 The 3D parameter space offers one novel approach to uncertainty analysis of global C cycle
591 models. As global land models incorporate more and more processes to simulate C cycle
592 responses to global change, it becomes very difficult to understand or evaluate complex model
593 behaviors. As such, differences in model projections cannot be easily diagnosed and attributed to
594 their sources (Chatfield, 1995; Friedlingstein et al., 2006; Luo et al., 2009). Eq. 7 can help
595 diagnose and evaluate complex models by placing all modeling results within one common
596 parameter space in spite of the fact that individual global models may have tens or hundreds of
597 parameters to represent C cycle processes as affected by many abiotic and biotic factors (Luo et
598 al., 2016). The 3D space can be used to measure how and how much the models diverge.

599 *Traceability analysis* The two terms on the right side of eq. 2 can be decomposed into
600 traceable components (Xia et al., 2013) so as to identify sources of uncertainty in C cycle model
601 projections. Model intercomparison projects (MIPs) all illustrate great spreads in projected land
602 C sink dynamics across models (Todd-Brown et al., 2013; Tian et al., 2015). It has been
603 extremely challenging to attribute the uncertainty to sources. Placing simulation results of a
604 variety of C cycle models within one common parameter space can measure how much the
605 model differences are in a common metrics (Eq. 7). The measured differences can be further
606 attributed to sources in model structure, parameter, and forcing fields with traceability analysis

Biogeosciences Discuss., doi:10.5194/bg-2016-377, 2016
Manuscript under review for journal Biogeosciences
Published: 16 September 2016

607 (Xia et al., 2013; Rafique et al., 2014; Ahlström et al., 2015; Chen et al., 2015). The traceability
608 analysis also can be used to evaluate effectiveness of newly incorporated modules into existing
609 models, such as adding the N module on simulated C dynamics (Xia et al., 2013) and locate the
610 origin of model ensemble uncertainties to external forcing vs. model structures and parameters
611 (Ahlström et al., 2015).

612 *Constrained estimates of terrestrial C sequestration* Traditionally, global land C sink is
613 indirectly estimated from airborne fraction of C emission and ocean uptake. Although many
614 global land models have been developed to estimate land C sequestration, a variety of MIPs
615 indicate that model predictions widely vary among them and do not fit observations well
616 (Schwalm et al., 2010; Luo et al., 2015; Tian et al., 2015). Moreover, the prevailing practices in
617 the modeling community, unfortunately, may not lead to significant enhancements in our
618 confidence on model predictions. For example, incorporating an increasing number of processes
619 that influence the C cycle may represent the real-world phenomena more realistically but makes
620 the models more complex and less tractable. MIPs have effectively revealed the extent of the
621 differences between model predictions (Schwalm et al., 2010; Keenan et al., 2012; De Kauwe et
622 al., 2013) but provide limited insights into sources of model differences (but see Medlyn et al.
623 (2015). The physical emulators make data assimilation computationally feasible for global C
624 cycle models Hararuk *et al*. (2014; 2015) and thus offer the possibility to generate independent
625 yet constrained estimates of global land C sequestration to be compared with the indirect
626 estimate. With the emulators, we can assimilate most of the C flux- and pool-related datasets into
627 those models to better constrain global land C sink dynamics.
628
629 **Concluding remarks**

Biogeosciences Discuss., doi:10.5194/bg-2016-377, 2016
Manuscript under review for journal Biogeosciences
Published: 16 September 2016

In this study we theoretically explored the transient dynamics of terrestrial C storage. Our analysis indicates that transient C storage dynamics can be partitioned into two components: the C storage capacity and the C storage potential. The capacity, which is the product of C input and residence time, represents their instantaneous responses to a state of external forcing at a given time. Thus, the C storage capacity quantifies the maximum amount of C that an ecosystem can store at the given environmental condition at a point of time. Thus it varies diurnally, seasonally, and interannually as environmental condition changes.

The C storage potential is the difference between the capacity and the current C storage and thus measures the magnitude of disequilibrium in the terrestrial C cycle (Luo and Weng, 2011). The storage potential represents the internal capability (or recovery force) of the terrestrial C cycle to influence the change in C storage in the next time step through redistribution of net C pool changes in a network of multiple pools with different residence times. The redistribution drives the current C storage towards the capacity and thus equilibrates C efflux with influx. We propose that the storage potential should be the targeted quantity for research, market trading, and government management for C credits.

The two components of land C storage dynamics represent interactions of external forces (via changes in the capacity) and internal capability of the land C cycle (via changes in the C storage potential) to generate complex phenomena of C cycle dynamics, such as fluctuations, directional changes, and tipping points, in the terrestrial ecosystems. From a system perspective, these complex phenomena are mostly caused by multiple environmental forcing variables interacting with relatively simple internal processes over different temporal and spatial scales. Note that while those internal processes can be mathematically represented with a relatively simple formula, their ecological and biological underpinnings can be very complex.

Biogeosciences Discuss., doi:10.5194/bg-2016-377, 2016
Manuscript under review for journal Biogeosciences
Published: 16 September 2016

653 The theoretical framework developed in this study has the potential to revolutionize
654 model evaluation. Our analysis indicates that the matrix equation as in eq. 1 or 2 can adequately
655 emulate most of the land C cycle models. Indeed, we have developed physical emulators of
656 several global land C cycle models. In addition, predictions of C dynamics with complex land
657 models can be placed in a 3D parameter space as a common metric to measure how much model
658 predictions are different. The latter can be traced to its source components by decomposing
659 model predictions to a hierarchy of traceable components. Moreover, the physical emulators
660 make it computationally possible to assimilate multiple sources of data to constrain predictions
661 of complex models.
662 The theoretical framework we developed in this study can well explain dynamics of C
663 storage in response to cyclic seasonal change in external forcings (e.g., Figs. 2 and 3) and climate
664 warming and rising atmospheric CO_2 (Fig. 5). It also can explain responses of ecosystem C
665 storage to disturbances and other global change factors, such as nitrogen deposition, land use
666 changes, and altered precipitation. The theoretical framework is simple and straightforward but
667 able to characterize the direction and rate of C storage change, which are arguably among the
668 most critical issues for quantifying terrestrial C sequestration. Future research should explicitly
669 incorporate stochastic disturbance regime shifts (e.g., Weng et al., 2012) and vegetation
670 dynamics (Moorcroft et al., 2001; Purves and Pacala, 2008; Fisher et al., 2010; Weng et al.,
671 2015) into this theoretical framework to explore their theoretical issues related to
672 biogeochemistry.
673
674
675 **Acknowledgements**: This work was partially done through the working group, Nonautonomous

676 Systems and Terrestrial Carbon Cycle, at the National Institute for Mathematical and Biological
677 Synthesis, an institute sponsored by the National Science Foundation, the US Department of
678 Homeland Security, and the US Department of Agriculture through NSF award no. EF-0832858,
679 with additional support from the University of Tennessee, Knoxville. Research in Yiqi Luo
680 EcoLab was financially supported by U.S. Department of Energy grants DE-SC0006982, DE-
681 SC0008270, DE-SC0014062, DE-SC0004601, and DE-SC0010715 and U.S. National Science
682 Foundation (NSF) grants DBI 0850290, EPS 0919466, DEB 0840964, and EF 1137293.

683

684 **References**

685 Adair, E. C., Parton, W. J., Del Grosso, S. J., Silver, W. L., Harmon, M. E., Hall, S. A., Burke, I.
686 C., and Hart, S. C.: Simple three-pool model accurately describes patterns of long-term litter
687 decomposition in diverse climates, Global Change Biol, 14, 2636-2660, 2008.

688 Ågren, G. I. and Bosatta, E.: Quality: A bridge between theory and experiment in soil organic
689 matter studies, Oikos, 76, 522-528, 1996.

690 Ahlström, A., Xia, J. Y., Arneth, A., Luo, Y. Q., and smith, B.: Importance of vegetation
691 dynamics for future terrestrial carbon cycling, Environmental Research Letters, 10, 054019
692 doi:054010.051088/051748-059326/054010/054015/054019, 2015.

693 Allison, S. D., Wallenstein, M. D., and Bradford, M. A.: Soil-carbon response to warming
694 dependent on microbial physiology, Nat Geosci, 3, 336-340, 2010.

695 Baldocchi, D., Falge, E., Gu, L. H., Olson, R., Hollinger, D., Running, S., Anthoni, P.,
696 Bernhofer, C., Davis, K., Evans, R., Fuentes, J., Goldstein, A., Katul, G., Law, B., Lee, X. H.,
697 Malhi, Y., Meyers, T., Munger, W., Oechel, W., U, K. T. P., Pilegaard, K., Schmid, H. P.,
698 Valentini, R., Verma, S., Vesala, T., Wilson, K., and Wofsy, S.: FLUXNET: A new tool to study
699 the temporal and spatial variability of ecosystem-scale carbon dioxide, water vapor, and energy
700 flux densities, B Am Meteorol Soc, 82, 2415-2434, 2001.

701 Bolker, B. M., Pacala, S. W., and Parton, W. J.: Linear analysis of soil decomposition: Insights
702 from the century model, Ecol Appl, 8, 425-439, 1998.

703 Borer, E. T., Harpole, W. S., Adler, P. B., Lind, E. M., Orrock, J. L., Seabloom, E. W., and
704 Smith, M. D.: Finding generality in ecology: a model for globally distributed experiments,
705 Methods in Ecology and Evolution, 5, 65-73, 2014.

706 Bosatta, E. and Ågren, G. I.: Dynamics of carbon and nitrogen in the organic matter of the soil: a
707 generic theory, American Naturalist, 1991. 227-245, 1991.

708 Burke, I. C., Yonker, C. M., Parton, W. J., Cole, C. V., Flach, K., and Schimel, D. S.: Texture,
709 Climate, and Cultivation Effects on Soil Organic-Matter Content in Us Grassland Soils, Soil Sci
710 Soc Am J, 53, 800-805, 1989.

711 Canadell, J. G., Le Quéré, C., Raupach, M. R., Field, C. B., Buitenhuis, E. T., Ciais, P., Conway,
712 T. J., Gillett, N. P., Houghton, R. A., and Marland, G.: Contributions to accelerating atmospheric
713 CO2 growth from economic activity, carbon intensity, and efficiency of natural sinks,
714 Proceedings of the National Academy of Sciences, 104, 18866-18870, 2007.

715 Caswell, H.: Prospective and retrospective perturbation analyses: their roles in conservation
716 biology, Ecology, 81, 619-627, 2000.

717 Chatfield, C.: Model uncertainty, data mining and statistical-inference, Journal of the Royal
718 Statistical Society Series a-Statistics in Society, 158, 419-466, 1995.

719 Chen, Y., Xia, J., Sun, Z., Li, J., Luo, Y., Gang, C., and Wang, Z.: The role of residence time in
720 diagnostic models of global carbon storage capacity: model decomposition based on a traceable
721 scheme, Scientific reports, 5, 2015.

722 Ciais, P., Gasser, T., Paris, J. D., Caldeira, K., Raupach, M. R., Canadell, J. G., Patwardhan, A.,
723 Friedlingstein, P., Piao, S. L., and Gitz, V.: Attributing the increase in atmospheric CO_2 to
724 emitters and absorbers, Nat Clim Change, 3, 926-930, 2013.

725 De Kauwe, M. G., Medlyn, B. E., Zaehle, S., Walker, A. P., Dietze, M. C., Hickler, T., Jain, A.
726 K., Luo, Y., Parton, W. J., Prentice, I. C., Smith, B., Thornton, P. E., Wang, S., Wang, Y.-P.,
727 Wårlind, D., Weng, E., Crous, K. Y., Ellsworth, D. S., Hanson, P. J., Seok Kim, H., Warren, J.
728 M., Oren, R., and Norby, R. J.: Forest water use and water use efficiency at elevated CO_2: a
729 model-data intercomparison at two contrasting temperate forest FACE sites, Global Change
730 Biology, 19, 1759-1779, 2013.

731 English, B. P., Min, W., Van Oijen, A. M., Lee, K. T., Luo, G., Sun, H., Cherayil, B. J., Kou, S.,
732 and Xie, X. S.: Ever-fluctuating single enzyme molecules: Michaelis-Menten equation revisited,
733 Nature chemical biology, 2, 87-94, 2006.

734 Exbrayat, J. F., Pitman, A. J., Zhang, Q., Abramowitz, G., and Wang, Y. P.: Examining soil
735 carbon uncertainty in a global model: response of microbial decomposition to temperature,
736 moisture and nutrient limitation, Biogeosciences, 10, 7095-7108, 2013.

737 Farquhar, G., von Caemmerer, S. v., and Berry, J.: A biochemical model of photosynthetic CO_2
738 assimilation in leaves of C3 species, Planta, 149, 78-90, 1980.

739 Fisher, R., McDowell, N., Purves, D., Moorcroft, P., Sitch, S., Cox, P., Huntingford, C., Meir, P.,
740 and Ian Woodward, F.: Assessing uncertainties in a second‐generation dynamic vegetation
741 model caused by ecological scale limitations, New Phytol, 187, 666-681, 2010.

742 Fraser, L. H., Henry, H. A., Carlyle, C. N., White, S. R., Beierkuhnlein, C., Cahill, J. F., Casper,
743 B. B., Cleland, E., Collins, S. L., and Dukes, J. S.: Coordinated distributed experiments: an
744 emerging tool for testing global hypotheses in ecology and environmental science, Frontiers in
745 Ecology and the Environment, 11, 147-155, 2013.

746 Friedlingstein, P., Cox, P., Betts, R., Bopp, L., Von Bloh, W., Brovkin, V., Cadule, P., Doney,
747 S., Eby, M., Fung, I., Bala, G., John, J., Jones, C., Joos, F., Kato, T., Kawamiya, M., Knorr, W.,
748 Lindsay, K., Matthews, H. D., Raddatz, T., Rayner, P., Reick, C., Roeckner, E., Schnitzler, K.
749 G., Schnur, R., Strassmann, K., Weaver, A. J., Yoshikawa, C., and Zeng, N.: Climate-carbon
750 cycle feedback analysis: Results from the (CMIP)-M-4 model intercomparison, J Climate, 19,
751 3337-3353, 2006.

752 Goetz, S. J., Bond-Lamberty, B., Law, B. E., Hicke, J. A., Huang, C., Houghton, R. A.,
753 McNulty, S., O'Halloran, T., Harmon, M., Meddens, A. J. H., Pfeifer, E. M., Mildrexler, D., and
754 Kasischke, E. S.: Observations and assessment of forest carbon dynamics following disturbance
755 in North America, J Geophys Res-Biogeo, 117, 2012.

756 Goldbeter, A.: Oscillatory enzyme reactions and Michaelis–Menten kinetics, FEBS letters, 587,
757 2778-2784, 2013.

758 Grosse, G., Harden, J., Turetsky, M., McGuire, A. D., Camill, P., Tarnocai, C., Frolking, S.,
759 Schuur, E. A. G., Jorgenson, T., Marchenko, S., Romanovsky, V., Wickland, K. P., French, N.,
760 Waldrop, M., Bourgeau-Chavez, L., and Striegl, R. G.: Vulnerability of high-latitude soil organic
761 carbon in North America to disturbance, J Geophys Res-Biogeo, 116, 2011.

762 Hammerling, D. M., Michalak, A. M., and Kawa, S. R.: Mapping of CO_2 at high spatiotemporal
763 resolution using satellite observations: Global distributions from OCO-2, J Geophys Res-Atmos,
764 117, do6306, 2012.

765 Hararuk, O., Smith, M. J., and Luo, Y. Q.: Microbial models with data-driven parameters predict
766 stronger soil carbon responses to climate change, Global Change Biology, 21, 2439-2453, 2015.

767 Hararuk, O., Xia, J. Y., and Luo, Y. Q.: Evaluation and improvement of a global land model
768 against soil carbon data using a Bayesian Markov chain Monte Carlo method, J Geophys Res-
769 Biogeo, 119, 403-417, 2014.

770 Harley, P., Thomas, R., Reynolds, J., and Strain, B.: Modelling photosynthesis of cotton grown
771 in elevated CO_2, Plant, Cell & Environment, 15, 271-282, 1992.

772 Hicke, J. A., Allen, C. D., Desai, A. R., Dietze, M. C., Hall, R. J., Hogg, E. H., Kashian, D. M.,
773 Moore, D., Raffa, K. F., Sturrock, R. N., and Vogelmann, J.: Effects of biotic disturbances on
774 forest carbon cycling in the United States and Canada, Global Change Biol, 18, 7-34, 2012.

775 Jenkinson, D., Hart, P., Rayner, J., and Parry, L.: Modelling the turnover of organic matter in
776 long-term experiments at Rothamsted, 1987. 1987.

Jones, C., McConnell, C., Coleman, K., Cox, P., Falloon, P., Jenkinson, D., and Powlson, D.: Global climate change and soil carbon stocks; predictions from two contrasting models for the turnover of organic carbon in soil, Global Change Biol, 11, 154-166, 2005.

Keenan, T. F., Baker, I., Barr, A., Ciais, P., Davis, K., Dietze, M., Dragoni, D., Gough, C. M., Grant, R., Hollinger, D., Hufkens, K., Poulter, B., McCaughey, H., Raczka, B., Ryu, Y., Schaefer, K., Tian, H., Verbeeck, H., Zhao, M., and Richardson, A. D.: Terrestrial biosphere model performance for inter-annual variability of land-atmosphere CO_2 exchange, Global Change Biol, 18, 1971-1987, 2012.

Kloeden, P. E. and Rasmussen, M.: Nonautonomous dynamical systems, American Mathematical Society, 2011.

Kloster, S., Mahowald, N. M., Randerson, J. T., Thornton, P. E., Hoffman, F. M., Levis, S., Lawrence, P. J., Feddema, J. J., Oleson, K. W., and Lawrence, D. M.: Fire dynamics during the 20th century simulated by the Community Land Model, Biogeosciences, 7, 2010.

Le Quéré, C., Moriarty, R., Andrew, R. M., Canadell, J. G., Sitch, S., Korsbakken, J. I., Friedlingstein, P., Peters, G. P., Andres, R. J., Boden, T. A., Houghton, R. A., House, J. I., Keeling, R. F., Tans, P., Arneth, A., Bakker, D. C. E., Barbero, L., Bopp, L., Chang, J., Chevallier, F., Chini, L. P., Ciais, P., Fader, M., Feely, R. A., Gkritzalis, T., Harris, I., Hauck, J., Ilyina, T., Jain, A. K., Kato, E., Kitidis, V., Klein Goldewijk, K., Koven, C., Landschützer, P., Lauvset, S. K., Lefèvre, N., Lenton, A., Lima, I. D., Metzl, N., Millero, F., Munro, D. R., Murata, A., Nabel, J. E. M. S., Nakaoka, S., Nojiri, Y., O'Brien, K., Olsen, A., Ono, T., Pérez, F. F., Pfeil, B., Pierrot, D., Poulter, B., Rehder, G., Rödenbeck, C., Saito, S., Schuster, U., Schwinger, J., Séférian, R., Steinhoff, T., Stocker, B. D., Sutton, A. J., Takahashi, T., Tilbrook, B., van der Laan-Luijkx, I. T., van der Werf, G. R., van Heuven, S., Vandemark, D., Viovy, N., Wiltshire, A., Zaehle, S., and Zeng, N.: Global Carbon Budget 2015, Earth Syst. Sci. Data, 7, 349-396, 2015.

Li, J. W., Luo, Y. Q., Natali, S., Schuur, E. A. G., Xia, J. Y., Kowalczyk, E., and Wang, Y. P.: Modeling permafrost thaw and ecosystem carbon cycle under annual and seasonal warming at an Arctic tundra site in Alaska, J Geophys Res-Biogeo, 119, 1129-1146, 2014.

Lloyd, J. and Taylor, J. A.: On the Temperature-Dependence of Soil Respiration, Funct Ecol, 8, 315-323, 1994.

Luo, Y., Ahlström, A., Allison, S. D., Batjes, N. H., Brovkin, V., Carvalhais, N., Chappell, A., Ciais, P., Davidson, E. A., Finzi, A., Georgiou, K., Guenet, B., Hararuk, O., Harden, J. W., He, Y., Hopkins, F., Jiang, L., Koven, C., Jackson, R. B., Jones, C. D., Lara, M. J., Liang, J., McGuire, A. D., Parton, W., Peng, C., Randerson, J. T., Salazar, A., Sierra, C. A., Smith, M. J., Tian, H., Todd-Brown, K. E. O., Torn, M., van Groenigen, K. J., Wang, Y. P., West, T. O., Wei, Y., Wieder, W. R., Xia, J., Xu, X., Xu, X., and Zhou, T.: Toward more realistic projections of soil carbon dynamics by Earth system models, Global Biogeochemical Cycles, 30, 40-56, 2016.

Luo, Y., Weng, E., Wu, X., Gao, C., Zhou, X., and Zhang, L.: Parameter identifiability, constraint, and equifinality in data assimilation with ecosystem models, Ecological Applications, 19, 571-574, 2009.

817 Luo, Y. and Zhou, X.: Soil respiration and the environment, Academic Press, Burlington, MA,
818 USA, 2006.

819 Luo, Y. Q., Keenan, T. F., and Smith, M.: Predictability of the terrestrial carbon cycle, Global
820 Change Biol, 21, 1737-1751, 2015.

821 Luo, Y. Q., Ogle, K., Tucker, C., Fei, S. F., Gao, C., LaDeau, S., Clark, J. S., and Schimel, D. S.:
822 Ecological forecasting and data assimilation in a data-rich era, Ecol Appl, 21, 1429-1442, 2011.

823 Luo, Y. Q. and Weng, E. S.: Dynamic disequilibrium of the terrestrial carbon cycle under global
824 change, Trends Ecol Evol, 26, 96-104, 2011.

825 Luo, Y. Q., White, L. W., Canadell, J. G., DeLucia, E. H., Ellsworth, D. S., Finzi, A. C., Lichter,
826 J., and Schlesinger, W. H.: Sustainability of terrestrial carbon sequestration: A case study in
827 Duke Forest with inversion approach, Global Biogeochem Cy, 17, 2003.

828 Manzoni, S. and Porporato, A.: Soil carbon and nitrogen mineralization: theory and models
829 across scales, Soil Biology and Biochemistry, 41, 1355-1379, 2009.

830 Matamala, R., Jastrow, J. D., Miller, R. M., and Garten, C. T.: Temporal changes in C and N
831 stocks of restored prairie: Implications for C sequestration strategies, Ecological Applications,
832 18, 1470-1488, 2008.

833 Medlyn, B. E., Zaehle, S., De Kauwe, M. G., Walker, A. P., Dietze, M. C., Hanson, P. J.,
834 Hickler, T., Jain, A. K., Luo, Y., Parton, W., Prentice, I. C., Thornton, P. E., Wang, S., Wang,
835 Y.-P., Weng, E., Iversen, C. M., McCarthy, H. R., Warren, J. M., Oren, R., and Norby, R. J.:
836 Using ecosystem experiments to improve vegetation models, Nature Climate Change, 5, 528-
837 534, 2015.

838 Moorcroft, P., Hurtt, G., and Pacala, S. W.: A method for scaling vegetation dynamics: the
839 ecosystem demography model (ED), Ecol Monogr, 71, 557-586, 2001.

840 Oleson, K., Lawrence, D., Bonan, G., Drewniak, B., Huang, M., Koven, C., Levis, S., Li, F.,
841 Riley, W., and Subin, Z.: Technical description of version 4.5 of the Community Land Model
842 (CLM), National Center for Atmospheric Research, Boulder, Colorado, 2013.

843 Olson, J. S.: Energy storage and the balance of producers and decomposers in ecological
844 systems, Ecology, 44, 322-331, 1963.

845 Pan, Y., Birdsey, R. A., Phillips, O. L., and Jackson, R. B.: The structure, distribution, and
846 biomass of the world's forests, Annual Review of Ecology, Evolution, and Systematics, 44, 593-
847 622, 2013.

848 Parton, W. J., Schimel, D. S., Cole, C. V., and Ojima, D. S.: Analysis of Factors Controlling Soil
849 Organic-Matter Levels in Great-Plains Grasslands, Soil Sci Soc Am J, 51, 1173-1179, 1987.

850 Parton, W. J., Scurlock, J. M. O., Ojima, D. S., Gilmanov, T. G., Scholes, R. J., Schimel, D. S.,
851 Kirchner, T., Menaut, J. C., Seastedt, T., Moya, E. G., Kamnalrut, A., and Kinyamario, J. I.:

852 Observations and Modeling of Biomass and Soil Organic-Matter Dynamics for the Grassland
853 Biome Worldwide, Global Biogeochem Cy, 7, 785-809, 1993.

854 Parton, W. J., Stewart, J. W. B., and Cole, C. V.: Dynamics of C, N, P and S in Grassland Soils -
855 a Model, Biogeochemistry, 5, 109-131, 1988.

856 Potter, C. S., Randerson, J. T., Field, C. B., Matson, P. A., Vitousek, P. M., Mooney, H. A., and
857 Klooster, S. A.: Terrestrial Ecosystem Production: a Process Model-Based on Global Satellite
858 and Surface Data, Global Biogeochem Cy, 7, 811-841, 1993.

859 Prentice, I. C., Kelley, D. I., Foster, P. N., Friedlingstein, P., Harrison, S. P., and Bartlein, P. J.:
860 Modeling fire and the terrestrial carbon balance, Global Biogeochem Cy, 25, 2011.

861 Purves, D. and Pacala, S.: Predictive models of forest dynamics, Science, 320, 1452-1453, 2008.

862 Rafique, R., Xia, J., Hararuk, O., and Luo, Y.: Structural analysis of three global land models on
863 carbon cycle simulations using a traceability framework, Biogeosciences Discussions, 11, 9979-
864 10014, 2014.

865 Rustad, L., Campbell, J., Marion, G., Norby, R., Mitchell, M., Hartley, A., Cornelissen, J., and
866 Gurevitch, J.: A meta-analysis of the response of soil respiration, net nitrogen mineralization,
867 and aboveground plant growth to experimental ecosystem warming, Oecologia, 126, 543-562,
868 2001.

869 Schwalm, C. R., Williams, C. A., Schaefer, K., Anderson, R., Arain, M. A., Baker, I., Barr, A.,
870 Black, T. A., Chen, G., Chen, J. M., Ciais, P., Davis, K. J., Desai, A., Dietze, M., Dragoni, D.,
871 Fischer, M. L., Flanagan, L. B., Grant, R., Gu, L., Hollinger, D., Izaurralde, R. C., Kucharik, C.,
872 Lafleur, P., Law, B. E., Li, L., Li, Z., Liu, S., Lokupitiya, E., Luo, Y., Ma, S., Margolis, H.,
873 Matamala, R., McCaughey, H., Monson, R. K., Oechel, W. C., Peng, C., Poulter, B., Price, D. T.,
874 Riciutto, D. M., Riley, W., Sahoo, A. K., Sprintsin, M., Sun, J., Tian, H., Tonitto, C., Verbeeck,
875 H., and Verma, S. B.: A model-data intercomparison of CO_2 exchange across North America:
876 Results from the North American Carbon Program site synthesis, Journal of Geophysical
877 Research: Biogeosciences, 115, n/a-n/a, 2010.

878 Sellers, P. J., Bounoua, L., Collatz, G. J., Randall, D. A., Dazlich, D. A., Los, S. O., Berry, J. A.,
879 Fung, I., Tucker, C. J., Field, C. B., and Jensen, T. G.: Comparison of radiative and physiological
880 effects of doubled atmospheric CO_2 on climate, Science, 271, 1402-1406, 1996.

881 Shi, Z., Yang, Y., Zhou, X., Weng, E., Finzi, A. C., and Luo, Y.: Inverse analysis of coupled
882 carbon–nitrogen cycles against multiple datasets at ambient and elevated CO2, J Plant Ecol, 9,
883 285-295, 2016.

884 Sierra, C. A. and Müller, M.: A general mathematical framework for representing soil organic
885 matter dynamics, Ecol Monogr, 85, 505-524, 2015.

886 Smith, J. U., Smith, P., Monaghan, R., and MacDonald, J.: When is a measured soil organic
887 matter fraction equivalent to a model pool?, Eur J Soil Sci, 53, 405-416, 2002.

888 Smith, P., Davis, S. J., Creutzig, F., Fuss, S., Minx, J., Gabrielle, B., Kato, E., Jackson, R. B.,
889 Cowie, A., and Kriegler, E.: Biophysical and economic limits to negative CO_2 emissions, Nat
890 Clim Change, 6, 42-50, 2016.

891 Stewart, C. E., Plante, A. F., Paustian, K., Conant, R. T., and Six, J.: Soil carbon saturation:
892 Linking concept and measurable carbon pools, Soil Sci Soc Am J, 72, 379-392, 2008.

893 Thonicke, K., Spessa, A., Prentice, I., Harrison, S. P., Dong, L., and Carmona-Moreno, C.: The
894 influence of vegetation, fire spread and fire behaviour on biomass burning and trace gas
895 emissions: results from a process-based model, Biogeosciences, 7, 1991-2011, 2010.

896 Tian, H. Q., Yang, Q. C., Najjar, R. G., Ren, W., Friedrichs, M. A. M., Hopkinson, C. S., and
897 Pan, S. F.: Anthropogenic and climatic influences on carbon fluxes from eastern North America
898 to the Atlantic Ocean: A process-based modeling study, J Geophys Res-Biogeo, 120, 752-772,
899 2015.

900 Todd-Brown, K. E. O., Randerson, J. T., Post, W. M., Hoffman, F. M., Tarnocai, C., Schuur, E.
901 A. G., and Allison, S. D.: Causes of variation in soil carbon simulations from CMIP5 Earth
902 system models and comparison with observations, Biogeosciences, 10, 1717-1736, 2013.

903 Walker, A. P., Aranda, I., Beckerman, A. P., Bown, H., Cernusak, L. A., Dang, Q. L.,
904 Domingues, T. F., Gu, L., Guo, S., Han, Q., Kattge, J., Kubiske, M., Manter, D., Merilo, E.,
905 Midgley, G., Porte, A., Scales, J. C., Tissue, D., Turnbull, T., Warren, C., Wohlfahrt, G.,
906 Woodward, F. I., and Wullschleger, S. D.: A Global Data Set of Leaf Photosynthetic Rates, Leaf
907 N and P, and Specific Leaf Area. Data set. Available on-line [http://daac.ornl.gov] from Oak
908 Ridge National Laboratory Distributed Active Archive Center, Oak Ridge, Tennessee, USA.
909 http://dx.doi.org/10.3334/ORNLDAAC/1224, 2014. 2014.

910 Wang, G. B., Zhou, Y., Xu, X., Ruan, H. H., and Wang, J. S.: Temperature Sensitivity of Soil
911 Organic Carbon Mineralization along an Elevation Gradient in the Wuyi Mountains, China, Plos
912 One, 8, 2013.

913 Wang, Y.-P. and Leuning, R.: A two-leaf model for canopy conductance, photosynthesis and
914 partitioning of available energy I:: Model description and comparison with a multi-layered
915 model, Agricultural and Forest Meteorology, 91, 89-111, 1998.

916 Wang, Y., Jiang, J., Chen-Charpentier, B., Agusto, F., Hastings, A., Hoffman, F., Rasmussen,
917 M., Smith, M., Todd-Brown, K., and Wang, Y.: Responses of two nonlinear microbial models to
918 warming and increased carbon input, Biogeosciences, 13, 887-902, 2016.

919 Wang, Y. P., Chen, B. C., Wieder, W. R., Leite, M., Medlyn, B. E., Rasmussen, M., Smith, M.
920 J., Agusto, F. B., Hoffman, F., and Luo, Y. Q.: Oscillatory behavior of two nonlinear microbial
921 models of soil carbon decomposition, Biogeosciences, 11, 1817-1831, 2014.

922 Weng, E. S. and Luo, Y. Q.: Soil hydrological properties regulate grassland ecosystem responses
923 to multifactor global change: A modeling analysis, J Geophys Res-Biogeo, 113, 2008.

924 Weng, E. S., Malyshev, S., Lichstein, J. W., Farrior, C. E., Dybzinski, R., Zhang, T.,
925 Shevliakova, E., and Pacala, S. W.: Scaling from individual trees to forests in an Earth system
926 modeling framework using a mathematically tractable model of height-structured competition,
927 Biogeosciences, 12, 2655-2694, 2015.

928 Weng, E. S. S., Luo, Y. Q., Wang, W. L., Wang, H., Hayes, D. J., McGuire, A. D., Hastings, A.,
929 and Schimel, D. S.: Ecosystem carbon storage capacity as affected by disturbance regimes: A
930 general theoretical model, J Geophys Res-Biogeo, 117, 2012.

931 West, T. O., Bandaru, V., Brandt, C. C., Schuh, A., and Ogle, S.: Regional uptake and release of
932 crop carbon in the United States, Biogeosciences, 8, 2037-2046, 2011.

933 Wieder, W. R., Bonan, G. B., and Allison, S. D.: Global soil carbon projections are improved by
934 modelling microbial processes, Nat Clim Change, 3, 909-912, 2013.

935 Xia, J. Y., Luo, Y. Q., Wang, Y. P., and Hararuk, O.: Traceable components of terrestrial carbon
936 storage capacity in biogeochemical models, Global Change Biol, 19, 2104-2116, 2013.

937 Xie, X. S.: Enzyme kinetics, past and present, Science, 342, 1457-1459, 2013.

938 Xu, X., Luo, Y. Q., and Zhou, J. Z.: Carbon quality and the temperature sensitivity of soil
939 organic carbon decomposition in a tallgrass prairie, Soil Biol Biochem, 50, 142-148, 2012.

940 Xu, X., Shi, Z., Li, D., Rey, A., Ruan, H. H., Craine, J. M., Liang, J., Zhou, J., and Luo, Y.: Soil
941 properties control decomposition of soil organic carbon: Results from data-assimilation analysis,
942 Geoderma, 262, 235-242, 2016.

943 Yang, Y. H., Luo, Y. Q., and Finzi, A. C.: Carbon and nitrogen dynamics during forest stand
944 development: a global synthesis, New Phytol, 190, 977-989, 2011.

945 Zhang, D. Q., Hui, D. F., Luo, Y. Q., and Zhou, G. Y.: Rates of litter decomposition in terrestrial
946 ecosystems: global patterns and controlling factors, J Plant Ecol, 1, 85-93, 2008.
947

948

949

Biogeosciences Discuss., doi:10.5194/bg-2016-377, 2016
Manuscript under review for journal Biogeosciences
Published: 16 September 2016

950 **Fig. 1** The Terrestrial ECOsystem (TECO) model and its outputs. Panels a is a schematic
951 representation of C transfers among multiple pools in plant, litter and soil in the TECO model.
952 TECO has feedback loops of C among soil pools. CWD = coarse wood debris, SOM = Soil
953 Organic Matter. Panel b compares the original TECO model outputs with those from matrix
954 equations for net ecosystem production (NEP = the sum of elements in $X'(t)$ from eq. 1). Panel
955 c compares the original TECO model outputs with those from matrix equations for ecosystem C
956 storage (= the sum of elements in $X(t)$ from eq. 2). The C storage values calculated with eq. 2
957 are close to 1:1 line with r^2 =0.998 with the modeled values (panel c). The minor mismatch in
958 estimated C storage between the matrix equation calculation and TECO outputs is due to
959 numerical errors via inverse matrix operation with some small numbers.
960
961 **Fig. 2** Seasonal cycles of the C storage capacity and C storage dynamics for the leaf pool (i.e.,
962 pool 1 as shown in Fig. 1). All the components are showed in panels b-d to calculate $x_{c,1}(t) =$
963 $b_1 u(t)\tau_1$ through multiplication, where $u(t) = NPP$ and $\tau_1 = 1/k_1$ for leaf.
964
965 **Fig. 3** Seasonal cycles of the C storage capacity and C storage dynamics for the litter pool (i.e.,
966 pool 4 as shown in Fig. 1). All the components are showed to calculate
967 $x_{c,4,u}(t) = \sum_{j=1}^{n} f_{4j}\,\tau_4 b_j u(t)$ in panels b-e and $x_{c,4,p}(t) = \sum_{j=1,j\neq 4}^{n} f_{4j}\,\tau_4 x'_j(t)$ in panels f-i for
968 litter. $x_{c,4,u}(t)$ is the maximal amount of C that can transfer from C input to the litter pool.
969 $x_{c,4,p}(t)$ is the maximal amount of C that can transfer from all the other pools to the litter pool.
970 This figure is to illustrate the network of pools through which C is distributed.
971

Biogeosciences Discuss., doi:10.5194/bg-2016-377, 2016
Manuscript under review for journal Biogeosciences
Published: 16 September 2016

Fig. 4 Components of the C storage capacity for litter pool (i.e., pool 4 as shown in Fig. 1). Component, $x_{c,4,u}(t)$, is the C from C input and component, $x_{c,4,p}(t)$, is the C from all the other pools to the litter pool. The sum of them is the attractor that determines the direction of C storage change in pool 4.

Fig. 5 Transient dynamics of ecosystem C storage in response to climate change in Harvard Forest. Panel a shows the time courses of the ecosystem C storage capacity, the ecosystem C storage potential, and ecosystem C storage (i.e., C stock) from 1850 to 2100. Panel b shows time courses of NPP(t) as C input and ecosystem residence times. Panel c shows correlated changes in ecosystem C storage potential and net ecosystem production (NEP). Panel d illustrates the regression between the C storage potential and NEP.

Fig. 6 The C storage capacity ($x_{c,i}(t)$), the C storage potential ($x_{p,i}(t)$), and C storage ($x_i(t)$) of individual pools. The potential is nearly zero for those fast turnover pools with short residence times but very large for those pools with long residence times.

Fig. 7 The C storage potential of individual pools ($x_{p,i}$) as influenced by net C pool change of different pools (x'_i) in their corresponding rows. The correlation coefficients show the degree of influences of net C pool change in one pool on the C storage potential of the corresponding pool through the network of C transfer. Those empty cells indicate no pathways of C transfer between those pools as indicated in Fig. 1.

Biogeosciences Discuss., doi:10.5194/bg-2016-377, 2016
Manuscript under review for journal Biogeosciences
Published: 16 September 2016

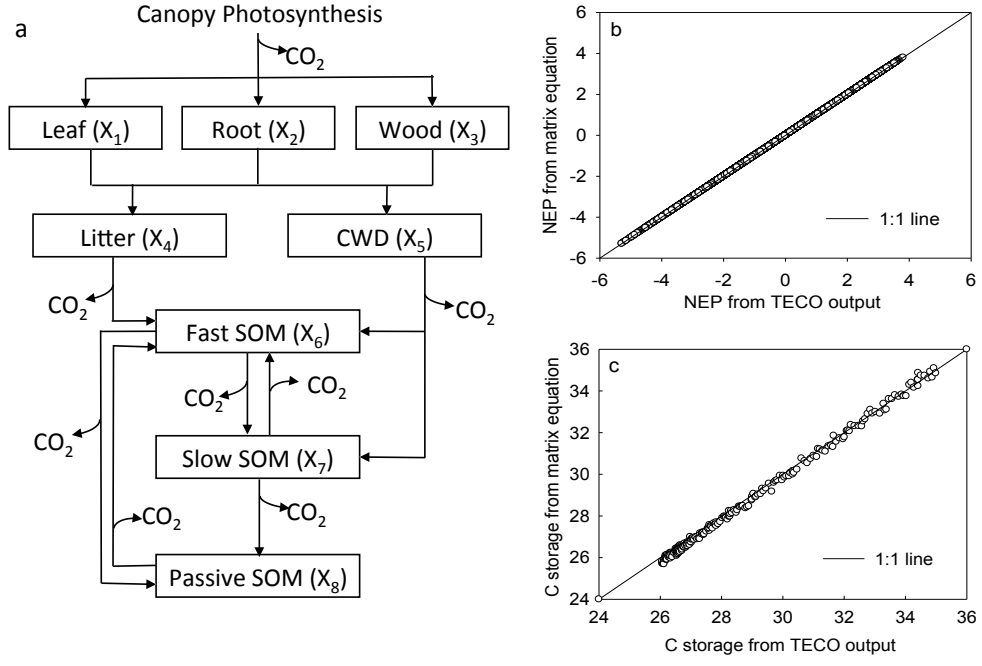

Fig. 1

Biogeosciences Discuss., doi:10.5194/bg-2016-377, 2016
Manuscript under review for journal Biogeosciences
Published: 16 September 2016

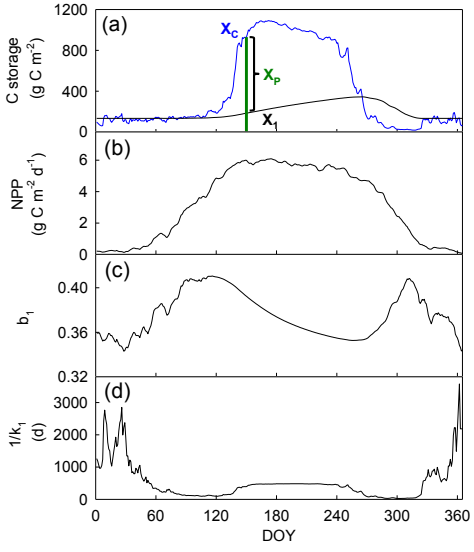

997
998
999
1000
1001
1002

Fig. 2

Biogeosciences Discuss., doi:10.5194/bg-2016-377, 2016
Manuscript under review for journal Biogeosciences
Published: 16 September 2016

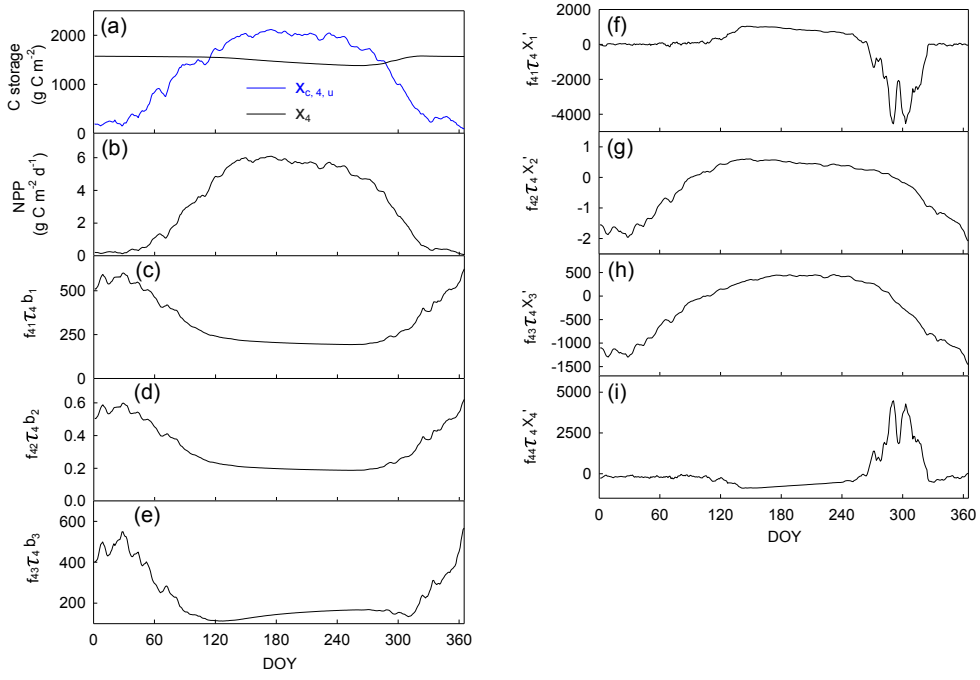

1003
1004 Fig. 3

Biogeosciences Discuss., doi:10.5194/bg-2016-377, 2016
Manuscript under review for journal Biogeosciences
Published: 16 September 2016

1005
1006

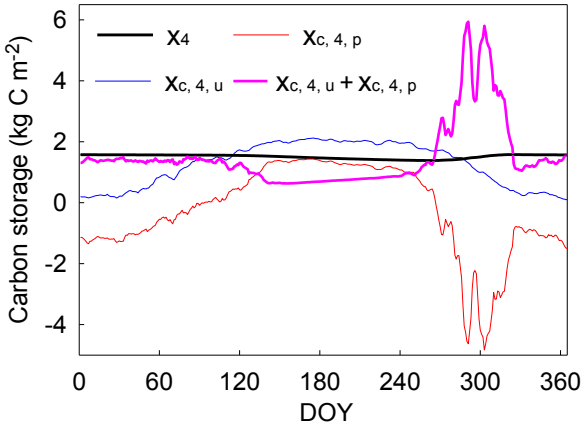

1007
1008
1009

Fig. 4

Biogeosciences Discuss., doi:10.5194/bg-2016-377, 2016
Manuscript under review for journal Biogeosciences
Published: 16 September 2016

1010

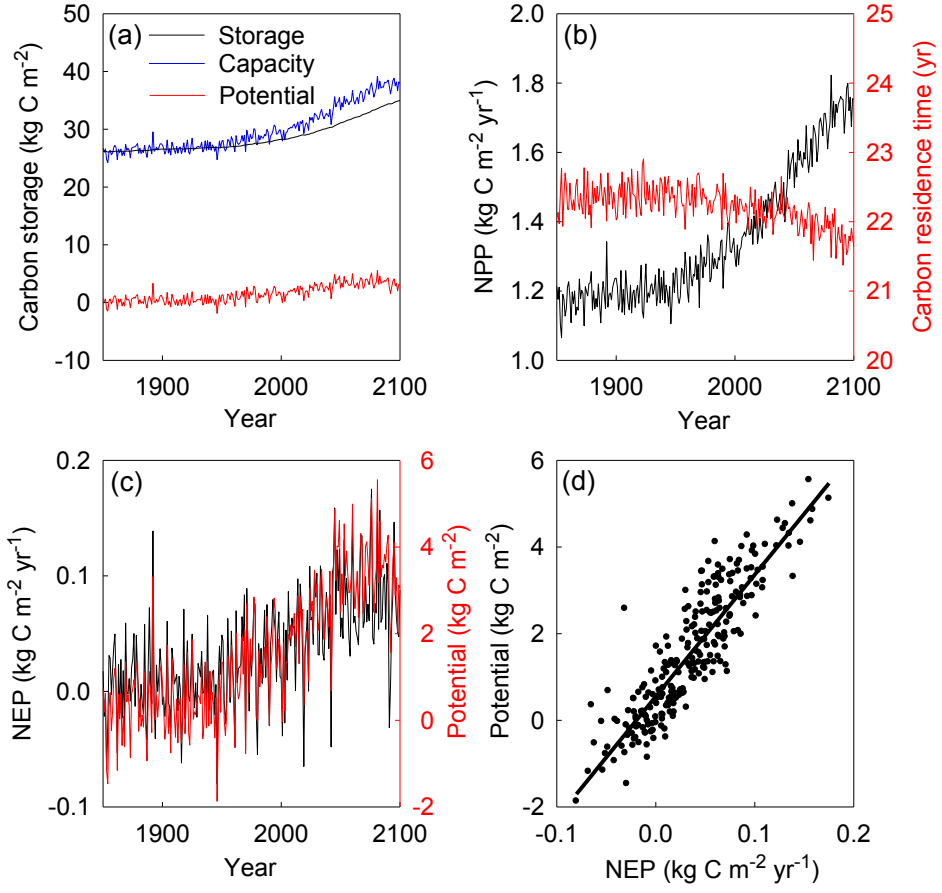

1011
1012
1013 Fig. 5
1014
1015

Biogeosciences Discuss., doi:10.5194/bg-2016-377, 2016
Manuscript under review for journal Biogeosciences
Published: 16 September 2016

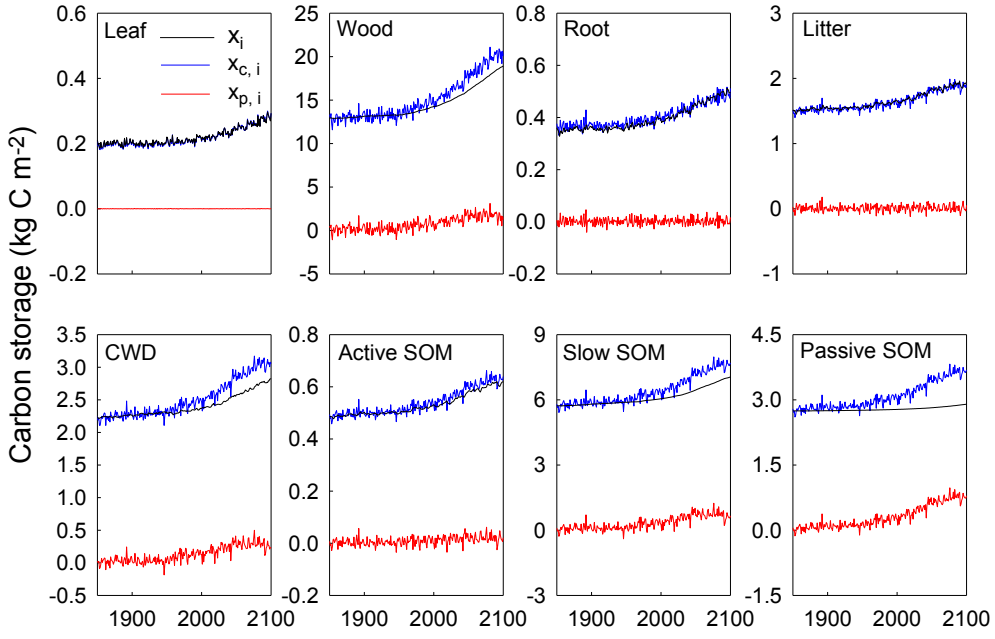

Fig. 6

Biogeosciences Discuss., doi:10.5194/bg-2016-377, 2016
Manuscript under review for journal Biogeosciences
Published: 16 September 2016

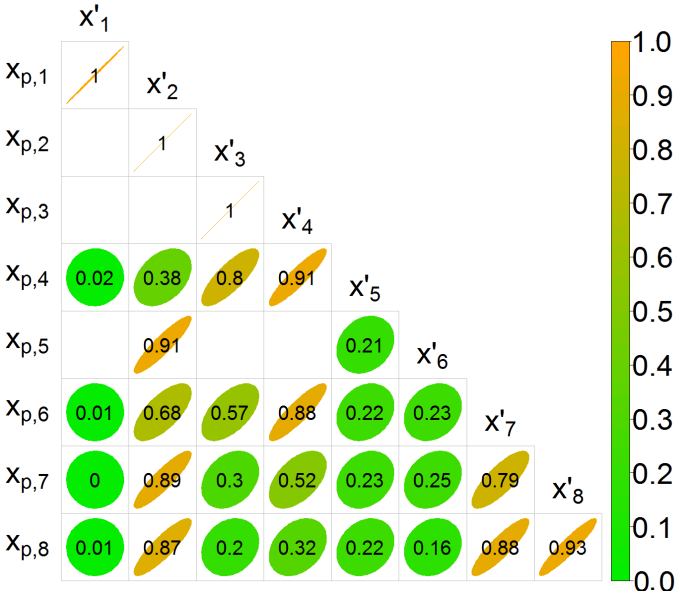

Fig. 7